Separation and Purification Technology 235 (2020) 116181

Contents lists available at ScienceDirect

Separation and Purification Technology

journal homepage: www.elsevier.com/locate/seppur

A multifunctional bi-phasic graphene oxide/chitosan paper for water treatment

Diego Cortinez[a], Patricia Palma[b], René Castro[a], Humberto Palza[a,c,*]

[a] Departamento de Ingeniería Química, Biotecnología y Materiales, Facultad de Ciencias Físicas y Matemáticas, Universidad de Chile, Chile
[b] Departamento de Patología y Medicina Oral, Facultad de Odontología, Universidad de Chile, Sergio Livingstone 943, Santiago, Chile
[c] Advanced Mining Technological Center, Facultad de Ciencias Físicas y Matemáticas, Universidad de Chile, Chile

ARTICLE INFO

Keywords:
Graphene oxide paper
Dye adsorption
Graphene oxide composite

ABSTRACT

A bi-phasic and water-stable GO paper was developed based on a simple casting method and the addition of a chitosan (CH) coating layer. While pure GO paper re-dispersed after water immersion water becoming a powder, the bi-phasic GO/CH paper presented water stability. The stable GO/CH paper was able to adsorb both anionic and cationic dyes showing a maximum monolayer adsorption capacity (q_m) of 103 mg/g and 232 mg/g for Methylene Blue and Methyl Orange, respectively. The biocidal behavior of GO and CH was rendered to the paper presenting antibacterial capacity against *Staphylococcus Aureus* and *Escherichia coli* under continuous agitation. These results show that our GO/CH paper can be a viable material for water treatment.

1. Introduction

Graphite oxide (GO) is a layered material consisting of hydrophilic oxygenated graphene sheets bearing functional groups on their basal planes and edges [1]. GO can be easily dispersed into a variety of solvents, such as water, due to presence of these functional groups that together with its planar structure makes it easy to assemble into paper-like morphologies [2]. GO papers have been obtained by various approaches including flow-directed filtration [1], evaporation-assembly [3], spin-coating [4], and Langmuir–Blodgett assembly [5]. The main property emerging from these papers relates with the mechanical behavior since they can exhibit superior stiffness and strength as compared with other paper-like carbon materials such as buckypaper and flexible graphite foil [2,3,6–8]. The hydrogen-bonding between the functional groups of the GO layers and water molecules explains the stiffness, flexibility and ductile behavior of these materials [7]. However, there is a limit for this hydrogen-bonding forming intersheet bridges and an excess of water molecules will both swell the structure and facilitate lateral "sliding" of the nanosheets [7]. The latter also means that a high amount of water molecules between the interlayers can produce a drop in the mechanical stiffness [1,7,9,10]. Indeed, GO films immersed in water are not stable as they are re-dispersed after mild shake or by standing for more than 24 h, resulting in a homogeneous suspension of GO particles [11]. Therefore, the applications of GO paper are limited to specific areas with well controlled humidity and water content.

Similar to other layered based film materials, most of reports about GO papers focus on the mechanical behavior and electrical conductivity despite the potential multifunctionality of the resulting graphene based structures [11]. For instance, GO membranes with tunable gas transport can be produced showing excellent gas selectivity through both specific interactions with the gases and the nanopores created by the edges of non-interlocked sheets formed within the structure [12,13]. Similar to GO particles [14], GO papers having silver nanoparticles can be used as bactericidal agent for water disinfection with the antimicrobial behavior coming from the metal nanoparticles [15]. A property still not explored in GO papers relates with the high ability of GO particles to adsorb different water pollutants such as dyes [16]. GO can be considered as an excellent water treatment agent because of its high surface area, large amount of activated functional groups, good dispersibility in water, relatively easy preparation methods, and biocompatibility [16,17]. GO showed a high affinity for positively charged molecules/ions because of its oxygen functional groups and, for instance, adsorption capacities of Methylene Blue (MB) between 150 and 714 mg/g were obtained depending on the specific GO used [16,18,19]. The adsorption capacity toward MB of GO increased exponentially by increasing its oxidation degree [16,20] as the electrostatic interaction is the primary binding strength between the pollutant and GO [21]. For aromatic adsorbates, π-π stacking interactions are the dominant driving force as found in DNA, porphyrin, and tetracyclines adsorption on GO

* Corresponding author at: Departamento de Ingeniería Química, Biotecnología y Materiales, Facultad de Ciencias Físicas y Matemáticas, Universidad de Chile, Chile.
E-mail address: hpalza@ing.uchile.cl (H. Palza).

https://doi.org/10.1016/j.seppur.2019.116181
Received 29 November 2018; Received in revised form 4 October 2019; Accepted 6 October 2019
Available online 09 October 2019
1383-5866/

[22–24]. Cation–π bonding can also contribute to the adsorption by a cation-induced polarization and electrostatic force between the cation and the permanent quadrupole of the π-electron-rich aromatic structure from GO [24]. Hydrogen bonds between hydroxy or carboxyl surface groups of GO, as a hydrogen electron donor, and oxygen atoms or aromatic rings of dye molecule, as electron acceptor, improve the adsorption capacity of GO [25]. Despite these outstanding results, GO papers for dye adsorption have not been reported, likely due to issues related with their water stability.

Unlike GO, natural biopolymers, such as polysaccharides, have been extensively studied as adsorbents for removal of dye molecules [26–28]. For instance, naturally cationic polysaccharides presented excellent levels of dye removal due to a combination of electrostatic attraction, van der Waals forces, and hydrogen bonding [26]. Even some non-polar biopolymers can also present good dye adsorption due to their greater hydrogen bonding [26]. To further improve the adsorption behavior of these polymers, nanocomposites are currently developed specially having carbon nanoparticles [29]. From the different biopolymers, chitosan is highlighted for dye adsorption due to its low cost and outstanding chelation behavior [30,31]. While GO presents adsorption capacities between 50 and 600 mg/g for cationic dyes depending on the oxidation degree [20], chitosan samples can present values as high as 2000 mg/g for anionic dyes [30]. Due to GO can also be used for adsorption of anionic dyes though hydrogen bonding and $\pi - \pi$ stacking forces [16], chitosan has been mixed with this nanoparticle to prepare either films, particles, fibers or hydrogel structures, presenting adsorption of both cationic and anionic dyes mainly through an electrostatic interaction [32–35]. The large surface area of GO improves the adsorption behavior of pure chitosan systems [34,35].

The goal of this contribution is to prepare water stable GO/chitosan papers by simple casting methods avoiding sophisticated instruments or vacuum-filtration techniques. In our methodology, a GO dispersion is casted and dry under ambient conditions, as reported previously [36,37], and afterward a casting of a chitosan (CH) solution was carried out on the surface of the slurry film allowing a bi-phasic GO/CH paper. After drying, this paper presented improved water stability allowing its use in adsorption of dyes and the elimination of bacteria due to the contribution of each phase. Our bi-phasic GO/CH paper is the first report of a composite biopolymer/GO taking advantage of the self-assembling capacity of GO for water treatment.

2. Methodology

2.1. Materials

Graphite (extra pure fine powder) with a particle size < 50 mm, sulfuric acid (98.08%, H2SO4), potassium permanganate (99%, KMnO4), hydrochloric acid (32%, HCl), and sodium nitrate (99.5%, NaNO3) were obtained from Merck (Germany) and used as received. Hydrogen peroxide (5%, H_2O_2) was purchased from Kadus S.A. Methyl orange (MO) and Methylene Blue (MB) dyes were purchased from Sigma Aldrich. Chitosan of medium molecular weight (50,000–190,000 [Da]) and with a 75–85% deacetylation was obtained from Sigma-Aldrich.

2.2. Synthesis of GO papers

The first step is an oxidation of graphite with $KMnO_4$ and $NaNO_3$ in concentrated sulphuric acid based on the Hummers and Offeman method [38]. This oxidation was carried out using 250 mL of concentrated sulfuric acid as dispersion medium per 10 g of graphite. To the stirred dispersion, 5 g of $NaNO_3$ was added and after 30 min of stirring, it was cooled down to 0 °C using an ice water bath. Then 30 g of $KMnO_4$ were slowly added during 4 h. When the addition was completed, the resulting dispersion was stirred at 35 °C for 1.5 h. The reaction was quenched by pouring the dispersion into a 500 mL solution of water increasing the temperature to around 95 °C and stirred during 30 min. Afterward, 400 mL of a solution of hydrogen peroxide at 10% was slowly added in order to remove excess of permanganate not reacted, and the mixture was stirred for 30 min at 60 °C. Finally, the agitation was stopped during 24 h to allow the sedimentation of the GO. To remove impurities from GO, a two steps process was carried out. First, GO solution was washed with hydrochloric acid to remove by-products and then cleaned with distilled water to remove the excess of acid, following the method described elsewhere [37]. After a sedimentation period of 24 h, the precipitated was washed by vacuum filtration using a paper filter (a mesh of 5 [μm]) with a solution of 400 [mL] of hydrochloric acid at 16%. At the end of this stage, the GO cake formed was dispersed in a 2000 mL beaker containing 1 L of distilled water using magnetic stirring for 15 [min]. The content of the beaker was settling during two days, and the supernatant was separated and centrifuged at 6000 [rpm] for 4 min, where only the highly exfoliated mud that settled was retained. The settled of the last process was washed with distilled water and was settling during two days where the supernatant is recovery and centrifuged at 6000 rpm for 4 min. Afterward, the precipitated was washed with 1 L of distilled water and centrifuged at 6000 RPM for 4 min. Finally, the last precipitated was washed with 1 L of distilled water and centrifuged at 9000 rpm for 20 min. The mud was recovered using a spoon and stored in a Petri dish for the paper preparation.

The GO mud from the purification process was spread out by a spatula of Teflon on a Teflon plate (polished using 1200 grit sandpaper) delimited by scotch-paper [37]. Afterward, a more humid GO mud was casted on that area using a micropipette, and allowed to dry for more than 24 h at room temperature until a paper was formed, which was then peeled out by using a metal spatula [39]. For the bi-phasic paper, the GO mud film obtained from the spread out process was dried for a short period (around 15 min) and then a solution at 2 v/v% of acetic acid having 10 mg/ml of chitosan was coated on the GO film and dried for 24 h.

2.3. Characterization

The samples were characterized by: Fourier Transform Infrared (FT-IR) in Agilent Cary 630 equipment having ATR accessory; and X-ray diffraction (XRD) analysis performed on a Siemens D-5000 diffractometer with scintillation detector diffraction system and Bragg–Brentano geometry operating with a Cu Kα1 radiation source filtered with a graphite monochromator (k = 1.5406 Å) at 40 kV and 30 mA in the 2 h range of 2–80° at a scan rate of 0.028/s. The zeta potential of the suspensions having the GO was measured using Particle Metrix equipment model Stabino.

For the maximum adsorption capacity over MB, between 2 and 8 mg of paper and between 6 and 16 mg of powder were added into four Falcon tubes containing 10 mL of the dye solution with concentrations ranging from 50 to 600 mg/L. The tubes were shaken for 24 h and centrifuged afterwards at 9000 RPM for 8 min. A small sample was taken from each tube and its dye concentration was calculated. For each adsorption value, a Perkin Elmer Lambda 650 UV–vis instrument equipped with a Praying Mantis and a Harrick powder cell was used at 660 nm and 465 nm, for MB and MO, respectively. The Langmuir and Freundlich models were used to obtain the main parameters related with the equilibrium adsorption as below explained.

The antibacterial contact (Kill kinetic assay) tests were based on a method reported previously using Gram-negative *Escherichia coli* (ATCC 25922) and *Staphylococcus aureus* (ATCC 25923) in continuous agitation. The *E. coli* and *S. Aureus* strains were grown in fresh Luria-Bertani (LB) and Tryptic Soy Broth (TSB), respectively, at 37 °C for 24 h. The bacterial suspensions were adjusted to reach the desired bacterial suspension of 10^8 CFU/ml. In the antibacterial assessment, 10 mL of the bacterial suspension was mixed with a square GO paper of 1×1 cm^2, or the equivalent GO powder in grams, and incubated overnight at

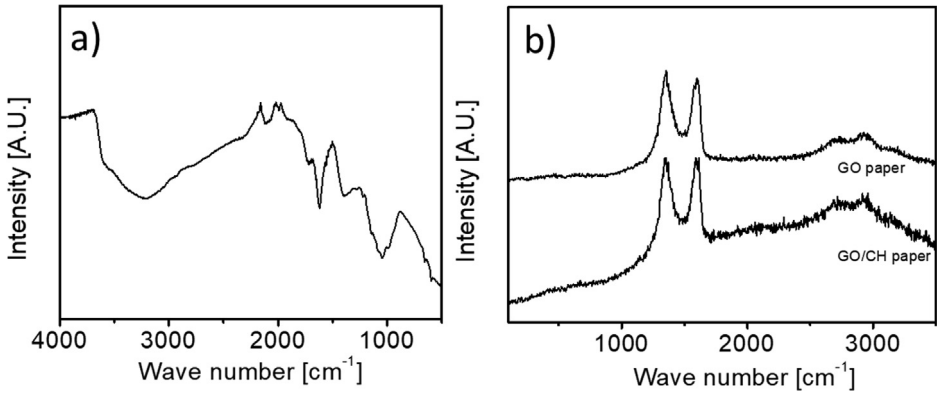

Fig. 1. Fourier transform infrared of the GO paper and Raman spectroscopy of GO and GO/CH papers.

37 °C using a rotary shaker. 100 µl aliquots of the final suspension were spread out and after different dilutions were plated out on TSA agar plates (triplicate). The antibacterial perform was calculate further using the reduction rate equation.

3. Results

The presence of oxygen groups in the GO due to the oxidation process of graphite was confirmed by FTIR as displayed in Fig. 1a. Pure GO paper showed the most characteristic GO structure bands at: 1717, 1604, and 1050 cm^{-1} corresponding to C═O stretching vibrations from carbonyl and carboxylic groups, skeletal vibrations from un-oxidized graphitic domains, and C−O stretching vibrations, respectively [40]. The broad band from the O−H stretching vibrations at 3430 cm^{-1} was further observed. The GO structure in the paper was further confirmed by Raman spectroscopy analyzing both the in-phase vibration of the graphite lattice (G band at 1575 cm^{-1}) and the disorder band caused by graphite defects (D band at 1355 cm^{-1}) as displayed in Fig. 1b [41]. With the oxidation process, the G band broadens displaying a shift to higher frequencies, and the D band grows in intensity. Indeed, the D- to G-band peak intensity ratio, I_D/I_G, is currently used to indicate defects in the GO structure that increases with the defects. The GO/CH paper shows a ratio of 1.50 meaning a high degree of defects in the GO structures. The pure GO paper presented a ratio of 1.44 meaning changes in the structures of GO by the presence of the chitosan film. An increase in this intensity ratio is indicative of the interaction of GO with CS as reported previously [42].

The structure of the papers was also analyzed by X-ray diffraction as displayed in Fig. 2. While original graphite presented a peak at 2θ = 26.3° from the (0 0 2) diffraction line of the natural flake, GO powder and papers presented a peak at low angles (around 11.4°) that is a further evidence of the oxidation process [43]. In papers based on polymer/GO composites a change in the interlayer distance can be found associated with adsorption of the polymer on the GO nanosheets [11]. In our case, the diffraction peak angle of GO particles is barely affected by either the paper process or the presence of the polymer, shifting from 11.2° for GO powder to 11.4° and 11.7° for the GO and GO/CH papers, respectively. This shift to higher angles and therefore to smaller interlayer distance can be associated with some reduction process during the dry of the GO paper and/or with the presence of chitosan acting as a reductant agent [11,44]. The GO/CH paper further presented two broad peaks at 2θ = 16.6° and 22.7° associated with the amorphous state of the chitosan film [39].

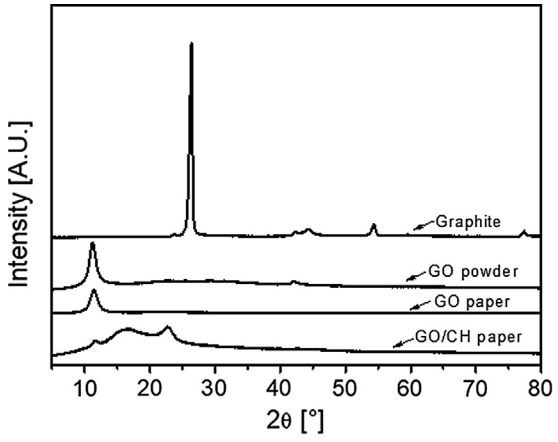

Fig. 2. X-ray diffractions of the different samples: original graphite, graphene oxide (GO) power, pure GO paper, and GO/CH paper.

Fig. 3 shows optical images of the samples prepared. Papers with sizes around 3 × 3 cm^2 were produced having excellent flexibility and manipulation, especially after the addition of a layer of chitosan on the GO paper. SEM images of the samples show a film having a thickness of around 10 µm with an ordered layer morphology associated with the high aspect ratio of the original GO particles (Fig. 4a and b). The high degree of anisotropy of the original GO dispersion allow the alignment in a specific direction driving the fabrication of self-aligned particle paper with a high degree of orientation [36]. However, our papers displayed a lower order and alignment as compared with previous results even under similar processing condition [1,24,36]. Indeed, individual GO sheets are not well compacted showing some waviness and interlayer gaps as previously reported [11]. Disorder structures in GO papers can be obtained by using smaller GO particles and structures with higher water content [45]. The lower the aspect ratio of GO particle, the worse is the alignment through the “excluded volume” interactions while the higher the amount of water content, the worse the compact structure. This tendency agree with our results as the lateral size of our GO particles in the paper is around some few micrometers (estimated by SEM micrographs) and its high amount of functional groups allows high water adsorption. The morphology of our paper seems to be in agreement with a semi-ordered accumulation mechanism where the adhesion between adjacent nanosheets is weak, producing a loosely aggregated structure with a roughly alignment increasing the interlayer distance [46]. By preparing GO paper by vacuum-assisted self-assembly process, the excess of solvent in this stage can be removed producing a second compressive phase reducing the spacing between nanosheets while orienting them parallel to the air-water interface. In our case, this last process is not produced explaining the morphology observed.

The casting process on the GO paper during the dry process produced a homogeneous and continues CH film of around 3 µm thickness (Fig. 4b). Regarding the interaction between chitosan and the GO paper, elemental analysis carried out by EDS to the bi-phasic GO/CH paper showed the presence of 13.2 w/w % of nitrogen atoms in the chitosan phase due to the presence of the biopolymer (Fig. 5a). On the

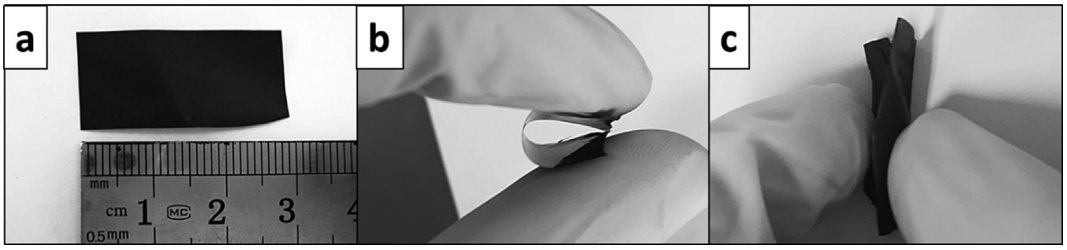

Fig. 3. Optical images of GO (a and b) and bi-phasic GO/CH (c) papers.

other hand, nitrogen atoms were not detected on the surface of the GO phase (Fig. 5b). However, on the lateral size of the GO phase of the bi-phasic paper (Fig. 5c) a 9.7 w/w % of nitrogen atoms was observed meaning that chitosan is presented in the structure of the GO phase. Therefore, chitosan molecules were able to present diffusion through the GO structure during the paper preparation.

The adsorption capacities of the papers were studied and quantified by the Langmuir and Freundlich models. The adsorption capacity at equilibrium was calculated by [47]:

$$q_e = \frac{(C_0 - C_e)V}{m} \quad (1)$$

where C_0 is the initial concentration, C_e is the concentration at equilibrium after being shaken the solution with the particles for 24 h and afterward centrifuged, V is the volume of the sample (in L), and m the mass of adsorbent used in the test (in g). From these concentrations of dyes adsorbed, the Langmuir isotherm in its linear form can be obtained:

$$\frac{C_e}{q_e} = \frac{1}{q_m K_L} + \frac{C_e}{q_m} \quad (2)$$

where q_m is the maximum adsorption capacity (mg/g) and K_L is the Langmuir constant related to the energy of adsorption (L/mg). The Freundlich isotherm otherwise could be represented as:

$$q_e = K_F \cdot C_e^n \quad (3)$$

where n and K_F ($mg^{1-n}L^n$)/g) are Freundlich parameters, in particular n is the adsorption strength; and K_F is generally related to the adsorption ability of the adsorbent when the value of the adsorbate concentration is equal to 1.

GO is a recognized good adsorbent agent for cationic dyes motivating us to characterize this behavior using Methylene Blue (MB) as a representative dye. Fig. 6 shows the adsorption isotherm of MB on the different papers and on GO powder showing both their capacity to adsorb the dye and that this process is highly depended of the material structure. GO powder was able to reach an asymptotic behavior at low dye concentrations (C_e) and with a high adsorption capacity (q_e). Pure GO paper presented a behavior as similar as GO particles regarding the high adsorption capacity although at higher dye concentrations. The similar behavior between the particle and the paper is explained by the poor water stability of the latter as a re-dispersion of GO particles from the paper after immersion in water was observed. Similar to other GO papers, the interaction between the paper and water molecules swells the paper structure and facilitates the lateral "sliding" of the carbon sheets [7,11]. Therefore, GO paper during the adsorption tests produced GO particles behaving as GO powder in adsorption (Fig. 6c). On the other hand, the GO/CH paper presented lower adsorption capacity as compared with pure GO paper as this structure was stable during the whole adsorption tests because of the chitosan/GO interactions as concluded by EDS analysis (Fig. 6d). The structure of GO/CH paper reduces the effective adsorption area as compared with GO powder explaining these results. The maximum adsorption capacity (q_m) and the Langmuir constant related to the energy of adsorption (K_L), together with the Freunlich parameters, are summarized in Table 1. While GO powder displayed a q_m = 322 mg/g, GO paper presented a value of 370 mg/g confirming the similar behavior between unstable paper and GO powder. It seems that the higher porosity of GO papers even when re-disperse increased the maximum adsorption capacity as compared with GO particles. GO/CH paper otherwise presented a q_m = 103 mg/g meaning that the paper structure allows a high adsorption of MB although lower than GO particles due to the chitosan film in one of the paper face reducing the adsorption area. The reduction process likely occurring on GO structures due to the presence of chitosan also can explain the lower adsorption capacity of the hybrid paper [20]. K_L constant from the Langmuir isotherm presented similar values between both papers although much lower as compared with GO particles. This parameter is related to the affinity of the binding sites meaning that isolated particles presented higher affinity to cation dyes than papers. The 1/n parameter from the Freundlich model is also displayed in Table 1 showing a value lower than 1 for the three materials indicating a Langmuir isotherm. Moreover, n gives an indication of how favorable is the process, confirming that GO particles have the highest value presenting therefore the best affinity for MB.

Based on the well-known adsorption capacity of chitosan compounds toward anionic dyes [30], the bi-phasic GO/CH paper was tested for adsorption of Methyl Orange as displayed in Fig. 7 and summarized in Table 1. The hybrid paper presented a maximum adsorption capacity (q_m) of 232.6 mg/g for MO that is even higher than the value for MB. In chitosan systems several mechanisms can explain

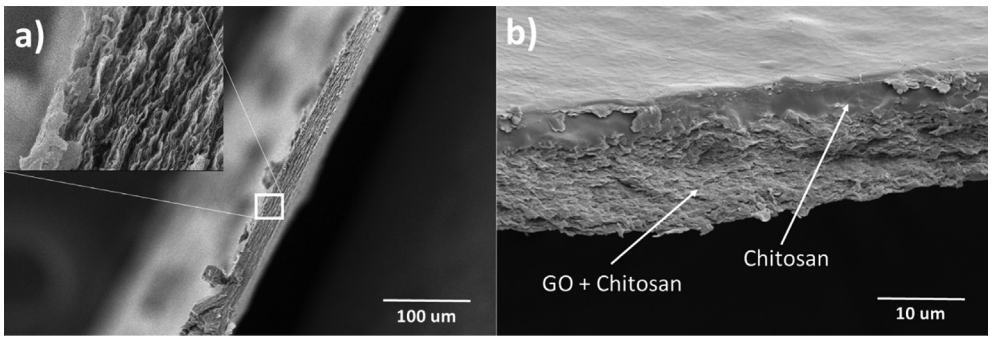

Fig. 4. Scanning electron images (SEM) from GO (a) and bi-phasic GO/CH (b) papers.

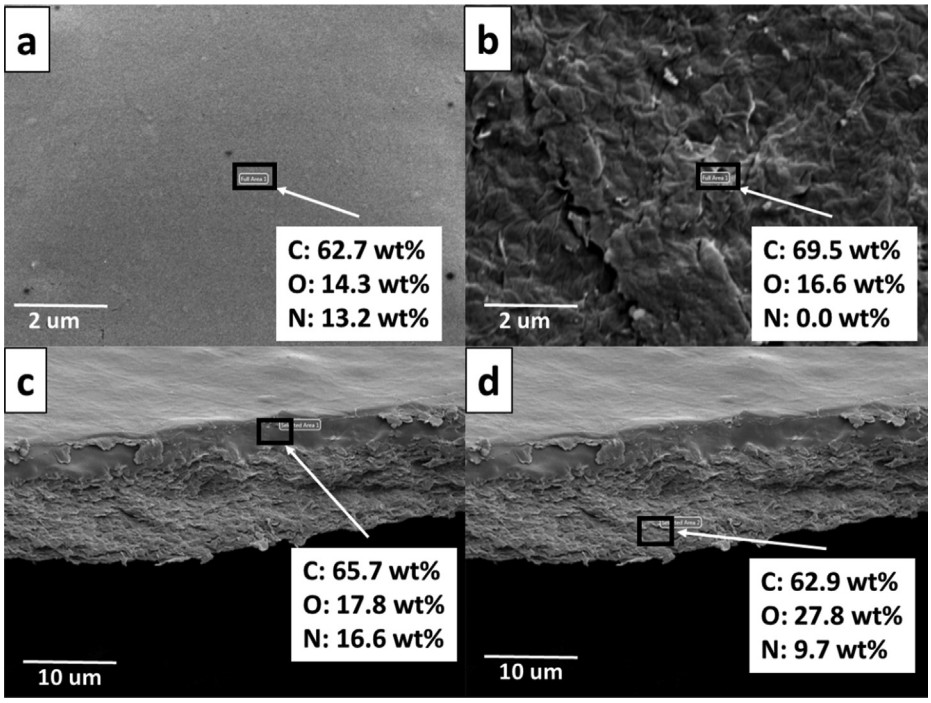

Fig. 5. Scanning electron images with the respective EDS analysis (black square) from the different areas of the bi-phasic GO/CH paper: (a) chitosan phase; (b) GO phase; (c) chitosan phase in the lateral area; and (d) GO phase in the lateral area.

the adsorption of dye such as those based on: surface adsorption, chemisorption, diffusion and adsorption-complexation theories. However, chemisorption is commonly cited as the main mechanism for the adsorption of anionic dyes where the amino groups from chitosan interact with the anionic dye [45]. Surface adsorption is another plausible mechanism by which dye molecules may be bound to chitosan, although likely both mechanisms acted simultaneously. However, the contribution of GO should also be considered in the adsorption of MO as depending on the oxidation level, GO adsorbs anionic dyes [16,48]. In this case, other mechanisms different from electrostatic interactions are involved such as hydrogen bonding and π-π stacking. Hydrogen bonds can occur between hydroxy or carboxyl surface groups of GO and oxygen atoms or aromatic rings from the dye molecule [16,25]. Table 1 further confirms that the adsorption of dyes in chitosan compounds is better fitted by Langmuir isotherm rather than Freundlich model [30,49].

Based on these results regarding the adsorption capacity of GO/CH paper for both anionic and cationic dyes, we can summarize the mechanisms involved depending on the characteristics of the dye. Cationic dyes, such as MB, can interact directly through electrostatic

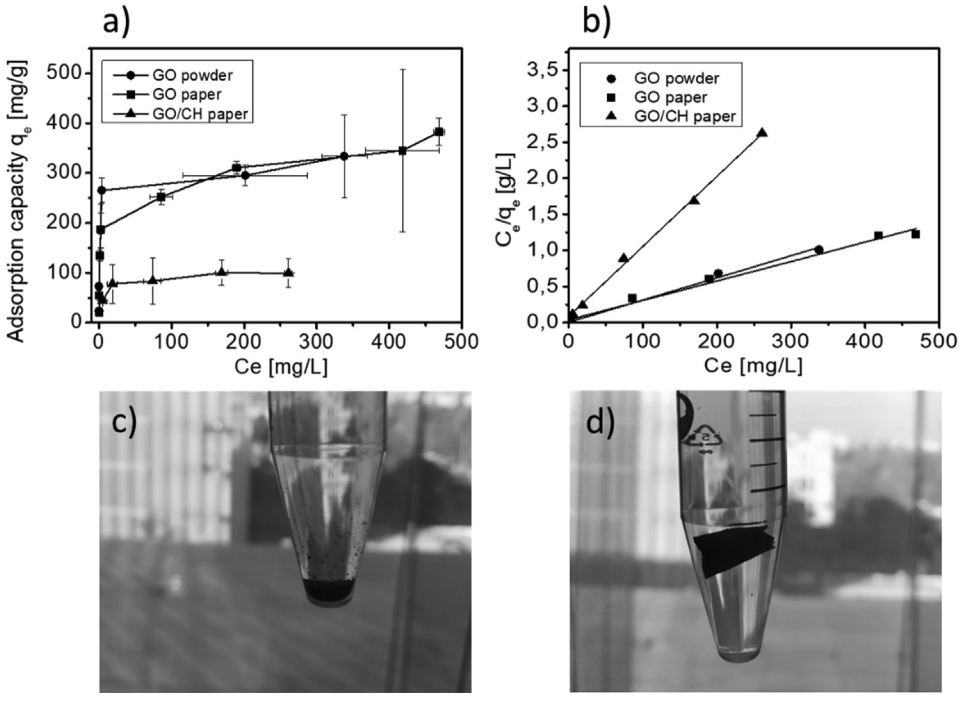

Fig. 6. (a) Langmuir adsorption isotherm of Methylene Blue (MB) on the different papers and on GO; and (b) its linear form; (c) optical image of the pure GO paper after the adsorption experiments showing the re-dispersion of GO particles precipitating at the bottom; and (d) optical image of the bi-phasic GO/CH paper that was stable during the whole adsorption experiment.

Table 1
Parameters from the Langmuir and Freundlich adsorption isotherms for the different samples studied. See equations 1–3 for details. The Freundlich constant has been assumed 1 in all cases. MB: Methylene Blue; MO: Methyl Orange.

Sample	Dye	Adsorption isotherm				
		Langmuir			Freundlich	
		q_m [mg/g]	K_L [L/mg]	R^2	1/n [–]	R^2
GO powder	MB	322.6	0.46	1.00	0.08	0.97
GO paper	MB	370.4	0.07	0.99	0.15	0.95
GO/CH paper	MB	103.1	0.11	1.00	0.19	0.87
GO/CH paper	MO	232.6	0.08	0.98	0.29	0.51

mechanisms with the negative surface charge of GO produced from its oxygen-based functional groups [16]. Negatively charged anionic dyes, such MO, can interact otherwise with the protonated amine groups from CH polymers also through long-distance electrostatic interactions from the presence of oppositely charge groups [30]. Hydrogen bonding can also explain, at least partially, the adsorption process in this case [30]. However, GO can also contribute to the adsorption of anionic dyes as the hydroxy or carboxyl groups from GO and the oxygen atoms or aromatic rings from the dye molecule can react through hydrogen bonds, the first as electron donor and the second as electron acceptor [16]. GO can also present a relevant proportion of graphene structures that can interact with the benzene rings and carbon double bonds from the dye by $\pi - \pi$ stacking [16,50]. Despite these results, the effect of the structure of each dye should be considered as it is one of the most important factors in adsorption processes [30]. The adsorption process can depend on the molecular size and the number of sulfonate groups of each dye although a correlation between adsorption and the structure of the dye is difficult to find [51]. For instance, in the adsorption of Acid Blue 9 and Food Yellow 3 dyes onto chitosan the main mechanism is the chemiosorption through the amino and hydroxyl groups of chitosan [52]. In this context, pH is a relevant variable that should be further considered in our discussion affecting the efficiency of adsorption through variations in the degree of ionisation of the adsorptive molecule and the adsorbent [53]. Chitosan is able to adsorb dyes under acidic and caustic conditions although with a mechanism that depends on pH [54]. For instance, pH affects the amine groups of chitosan that allow the adsorption through an electrostactic attraction [30]. By decreasing the pH, more protons are available to protonate the amine group of chitosan increasing therefore the dye adsorption through electrostatic interactions [30]. Under caustic conditions the covalent bonding of dye and the hydroxyl groups of chitosan further contribute to the adsorption together with both physical and chemical adsorption mechanisms [54]. These mechanisms explain the stability of a protonated cross-linked chitosan in removing MO in a wide range of pH (from 1.0 to 9.1) [55].

Table 2
Dye adsorptions (MB and MO) of our GO/CH bi-phasic paper as compared with other similar systems previously reported.

Sample	Dye	q_e [mg/g]
GO	MB	476.2–312.5 [16]
GO	MB	48.8–598.8 [20]
GO	MB	1939 [56]
GO	MB	17.3 [48]
GO	MB	223.8 [57]
GO/CH/β-cyclodextrin	MB	84.3 [35]
GO/CH	MB	468 [32]
GO/CH paper	MB	103 [this work]
GO	MO	105.3–263.2 [16]
CH	MO	180.2 [55]
GO	MO	16.8 [58]
GO/CH paper	MO	232 [this work]

Table 2 shows a summary of the equilibrium adsorption values found in our GO/CH paper as compared with similar systems previously published for the same dyes. This table confirms that our paper is a good candidate for adsorption of dyes with values between those reported for pure GO particles and other CH/GO systems. For instance, our results for MB adsorption were lower than the values from the CH/GO composite prepared by Yeng et al. although higher than GO/CH/β-cyclodextrin compound prepared by Fan et al [32,35]. For MO dye, our paper presents even better results showing one of the highest values, that is only lower than pure GO particles. Based on these results, we can state that the advantage of our system relate with its capacity to adsorb both cationic and anionic dyes and the its structure facilitating the posterior separation.

Motivated by the outstanding antibacterial behavior of both GO particles and chitosan films, the capacity of the different samples to kill Gram-positive *Staphylococcus Aureus* and Gram-negative *Escherichia coli* bacteria was tested [59,60]. These results, together with the behavior of a chitosan film and GO powder, are displayed in Fig. 8 confirming the antimicrobial behavior of the different papers. Pure and bi-phasic GO papers were able to kill *S. Aureus* and *E. coli* with a reduction around 54 and 25%, respectively, without a relevant effect of the type of paper. The presence of an additional outer membrane in Gram-negative *E. coli* bacteria explains its higher resistance to the toxicity of GO papers as reported previously in GO powders [61]. The antimicrobial behavior of GO arises from the bacteria disruption caused by the contact with these nanoparticles under different mechanisms as recently reviewed [62]. One mechanism is based on the bacterial membrane stress meaning a physical disruption of the membrane by the GO particles while another mechanism is based on oxidative stress. Despite these antecedents, pure chitosan film presented the highest antimicrobial activity coming from its polycationic structure allowing electrostatic interaction with the predominantly anionic components of the bacteria surface [60]. However, the high antimicrobial behavior of chitosan did not add any

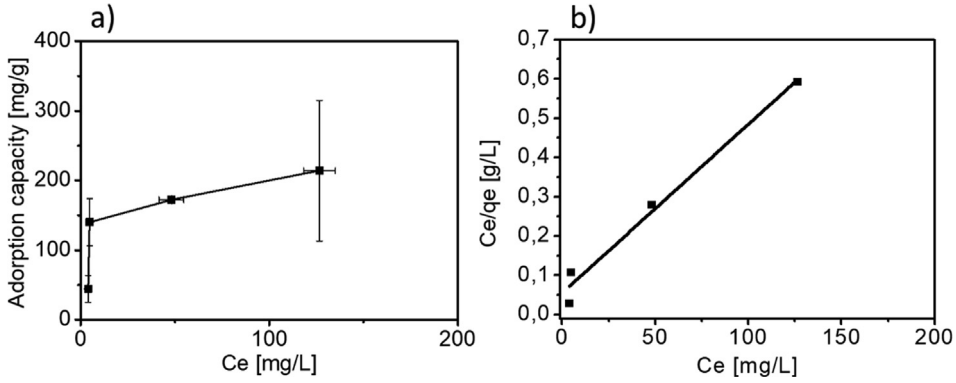

Fig. 7. (a) Langmuir adsorption isotherm of Methyl Orange (MO) on the bi-phasic GO/CH paper and (b) its linear form.

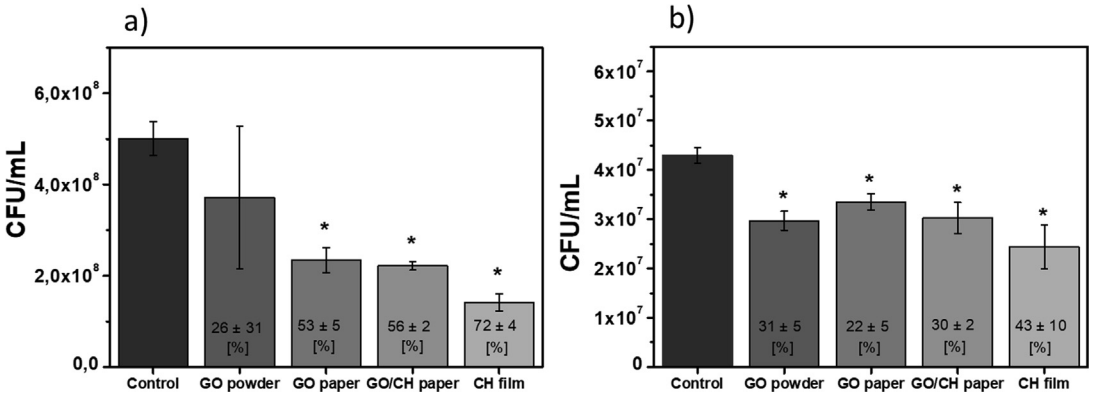

Fig. 8. Antibacterial behavior of the different samples capacity against *Staphylococcus Aureus* (a) and *Escherichia coli* (b). * represent a significant statistical difference between the result and control ($p < 0.05$).

synergic effect to the GO structures.

These results show that our novel CH/GO paper can be used for water treatment as it can adsorb cationic and anionic dyes further killing microorganisms, with high water stability overcoming some limitations of standard graphene based papers. However, similar to other materials based on carbon nanostructures, such as nanotubes and graphene particles, environmental issues should be considered either for the potential risks or for their effect on the adsorption processes [63–66]. For instance, the increasing demand for these particles will trigger a mass accumulation in soil and sediment due to their release into the environment. Under these conditions, the high adsorption of these carbon structures can generate issues related with resuspensions, changes in the metabolic function of sediment microbial communities, and modifications of the adsorption capacity of the sediment itself [65]. To our knowledge, these environmental studies have not yet been carried out for graphene paper structures although based on the large effect of water is hypothesized that the behavior will be as similar graphene based particles. Another point that should be analyzed for the real application of our CH/GO paper relates with the scaling up process, not only for the paper preparation but also for the treatment of large amount of water as dense films are not the most used materials for adsorption processes. However, our methodology is based on a low cost process using a cheap biopolymer such as chitosan, where the only expensive compound is GO that should become cheaper in the long-term as similar as the price evolution of carbon nanotubes [67].

4. Conclusions

A bi-phasic GO/CH paper was produced by a simple casting process allowing to improve its water stability as compared with pure GO paper. The bi-phasic paper was characterized by a GO layer thickness of around 10 μm and a homogeneous CH thickness of 3 μm. EDS analysis showed that CH molecules were able to diffuse through the GO layer explaining the water stability of the paper. The bi-phasic GO/CH structure was able to adsorb Methylene Blue (cationic dye) with a maximum monolayer adsorption capacity (q_m) of 103 mg/g meanwhile pure GO paper re-disperse during the adsorption tests with a behavior as similar as GO powder. The bi-phasic paper was further able to adsorb Methyl Orange (anionic dye) with a maximum adsorption capacity of 232 mg/g due to the contribution of each phase. The antimicrobial behavior of GO and CH was rendered to the papers presenting antibacterial capacity against *Escherichia coli* and *Staphylococcus Aureus*, with a higher toxicity for the latter strains. The improved water stability of our bi-phasic GO/CH paper material can be used to take advantage of the functionalities of each component allowing future design of membranes for water treatment.

Declaration of Competing Interest

On behalf of all the authors associated with this publication, I declare that we do not have any conflict of interest concerning any results or funding associated with it.

Acknowledgments

The authors gratefully acknowledge the financial support of CONICYT under FONDECYT Project 1150130 and Fondequip EQM150101. This work was also funded by the CONICYT/PIA Project AFB180004.

References

[1] D.A. Dikin, S. Stankovich, E.J. Zimney, R.D. Piner, G.H.B. Dommett, G. Evmenenko, S.T. Nguyen, R.S. Ruoff, Preparation and characterization of graphene oxide paper, Nature 448 (2007) 457.
[2] Y. Gao, L.Q. Liu, S.Z. Zu, K. Peng, D. Zhou, B.H. Han, Z. Zhang, The effect of interlayer adhesion on the mechanical behaviors of macroscopic graphene oxide papers, ACS Nano 5 (2011) 2134.
[3] C.M. Chen, Q.H. Yang, Y.G. Yang, W. Lv, Y.F. Wen, P.X. Hou, et al., Self-assembled free-standing graphite oxide membrane, Adv. Mater. 21 (2009) 3007.
[4] Z.T. Luo, Y. Lu, L.A. Somers, A.T.C. Johnson, High yield preparation of macroscopic graphene oxide membranes, J. Am. Chem. Soc. 131 (2009) 898.
[5] D.D. Kulkarni, I. Choi, S.S. Singamaneni, V.V. Tsukruk, Graphene oxide- polyelectrolyte nanomembranes, ACS Nano 4 (2010) 4667.
[6] Y. Su, H. Wei, R. Gao, Z. Yang, J. Zhang, Z. Zhong, Y. Zhang, Exceptional negative thermal expansion and viscoelastic properties of graphene oxide paper, Carbon 50 (2012) 2804.
[7] O.C. Compton, S.W. Cranford, K.W. Putz, Z. An, L.C. Brinson, M.J. Buehler, S.B.T. Nguyen, Tuning the mechanical properties of graphene oxide paper and its associated polymer nanocomposites by controlling cooperative intersheet hydrogen bonding, ACS Nano 6 (2012) 2008.
[8] N.V. Medhekar, A. Ramasubramaniam, R.S. Ruoff, V.B. Shenoy, Hydrogen bond networks in graphene oxide composite paper: structure and mechanical properties, ACS Nano 4 (2010) 2300.
[9] S. Park, J. An, J.W. Suk, R.S. Ruoff, Graphene-based actuators, Small 6 (2010) 210.
[10] A. Lerf, A. Buchsteiner, J. Pieper, S. Schottl, I. Dekany, T. Szabo, H.P. Boehm, Hydration behavior and dynamics of water molecules in graphite oxide, J. Phys. Chem. Solids. 67 (2006) 1106.
[11] Y.Q. Li, T.T. Yu, Y. Yang, L.X. Zheng, K. Liao, Bio-inspired nacre-like composite films based on graphene with superior mechanical, electrical, and biocompatible properties, Adv. Mater. 24 (2012) 3426.
[12] H.W. Kim, H.W. Yoon, S.M. Yoon, B.M. Yoo, B.K. Ahn, Y.H. Cho, H.J. Shin, H. Yang, U. Paik, S. Kwon, J.Y. Choi, H.B. Park, Selective gas transport through few-layered graphene and graphene oxide membranes, Science 342 (2013) 91.
[13] H. Li, Z. Song, X. Zhang, Y. Huang, S. Li, Y. Mao, H.J. Ploehn, Y. Bao, M. Yu, Ultrathin, molecular-sieving graphene oxide membranes for selective hydrogen separation, Science 342 (2013) 95.
[14] C. Angulo-Pineda, P. Palma, J. Bejarano, A. Riveros, M. Kogan, H. Palza, Antibacterial silver nanoparticles supported on graphene oxide with reduced cytotoxicity, JOM 79 (2019) 3698–3705.
[15] Q. Bao, D. Zhang, P. Qi, Synthesis and characterization of silver nanoparticle and graphene oxide nanosheet composites as a bactericidal agent for water disinfection, J. Colloid Interface Sci. 360 (2011) 463.
[16] C. Zolezzi, C. Ihle, C. Angulo, P. Palma, H. Palza, Effect of the oxidation degree of graphene oxides on their adsorption, flocculation and antibacterial behavior, Ind.

Eng. Chem. Res. 57 (2018) 15722–15730.
[17] Z. Yang, H. Yan, H. Yang, H. Li, A. Li, R. Cheng, Flocculation performance and mechanism of graphene oxide for removal of various contaminants from water, Water Res. 47 (2013) 3037.
[18] S.T. Yang, S. Chen, Y. Chang, A. Cao, Y. Liu, H. Wang, Removal of methylene blue from aqueous solution by graphene oxide, J. Colloid Interface Sci. 359 (2011) 24.
[19] T. Liu, Y. Li, Q. Du, J. Sun, Y. Jiao, G. Yang, Z. Wang, Y. Xia, W. Zhang, K. Wang, H. Zhu, D. Wu, Adsorption of methylene blue from aqueous solution by graphene, Colloids Surfaces B: Biointerf. 90 (2012) 197.
[20] H. Yan, X. Tao, Z. Yang, K. Li, H. Yang, A. Li, R. Cheng, Effects of the oxidation degree of graphene oxide on the adsorption of methylene blue, J. Hazardous Mat. 268 (2014) 191.
[21] T. Hartono, S.B. Wang, Q. Ma, Z.H. Zhu, Layer structured graphite oxide as a novel adsorbent for humic acid removal from aqueous solution, J. Colloids Interface Sci. 333 (2009) 114.
[22] S. He, B. Song, D. Li, C. Zhu, W. Qi, Y. Wen, L. Wang, S. Song, H. Fang, C. Fan, A graphene nanoprobe for rapid, sensitive, and multicolor fluorescent DNA analysis, Adv. Funct. Mater. 20 (2010) 453.
[23] J. Geng, H.T. Jung, Porphyrin functionalized graphene sheets in aqueous suspensions: from the preparation of graphene sheets to highly conductive graphene films, J. Phys. Chem. C. 114 (2010) 8227.
[24] Y. Gao, Y. Lia, L. Zhang, H. Huang, J. Hua, S.M. Shah, X. Su, Adsorption and removal of tetracycline antibiotics from aqueous solution by graphene oxide, J. Colloid Interface Sci. 368 (2012) 540.
[25] W. Konicki, M. Aleksandrzak, D. Moszyński, E. Mijowsk, Adsorption of anionic azo-dyes from aqueous solutions onto graphene oxide: Equilibrium, kinetic and thermodynamic studies, J. Colloid Interface Sci. 496 (2017) 188.
[26] R.S. Blackburn, Natural polysaccharides and their interactions with dye molecules: applications in effluent treatment, Environ. Sci. Technol. 38 (2004) 4905.
[27] H. Tu, Y. Yu, J. Chen, X. Shi, J. Zhou, H. Deng, Y. Du, Highly cost-effective and high-strength hydrogels as dye adsorbents from natural polymers: chitosan and cellulose, Polym. Chem. 8 (2017) 2913.
[28] T. Lu, T. Xiang, X.L. Huang, C. Li, W.F. Zhao, Q. Zhang, C.S. Zhao, Post-crosslinking towards stimuli-responsive sodium alginate beads for the removal of dye and heavy metals, Carbohydr. Polym. 133 (2015) 587.
[29] K. Sui, Y. Li, R. Liu, Y. Zhang, X. Zhao, H. Liang, Y. Xia, Biocomposite fiber of calcium alginate/multi-walled carbon nanotubes with enhanced adsorption properties for ionic dyes, Carbohydr. Polym. 90 (2012) 399.
[30] G. Crini, P.M. Badot, Application of chitosan, a natural aminopolysaccharide, for dye removal from aqueous solutions by adsorption processes using batch studies: A review of recent literature, Prog. Polym. Sci. 33 (2008) 399.
[31] W.S.W. Ngah, L.C. Teong, M.A.K.M. Hanafiah, Adsorption of dyes and heavy metal ions by chitosan composites: A review, Carbohydr. Polym. 83 (2011) 1446.
[32] S.T. Yang, J. Luo, J.H. Liu, Q. Zhou, J. Wan, C. Ma, R. Liao, H. Wang, L. Haifang, Y. Liu, Graphene oxide/chitosan composite for methylene blue adsorption, Nanosci. Nanotechnol. Lett. 5 (2013) 372.
[33] Y. Chen, L. Chen, H. Bai, L. Li, Graphene oxide–chitosan composite hydrogels as broad-spectrum adsorbents for water purification, J. Mater. Chem. A 1 (2013) 1992.
[34] Q. Du, J. Sun, Y. Li, X. Yang, X. Wang, Z. Wang, L. Xia, Highly enhanced adsorption of congo red onto graphene oxide/chitosan fibers by wet-chemical etching off silica nanoparticles, Chem. Eng. J. 245 (2014) 99.
[35] L. Fan, C. Luo, M. Sun, H. Qiu, X. Li, Synthesis of magnetic β-cyclodextrin–chitosan/graphene oxide as nanoadsorbent and its application in dye adsorption and removal, Colloids Surfaces B: Biointerf. 103 (2013) 601.
[36] S.H. Aboutalebi, M.M. Gudarzi, Q.B. Zheng, J.K. Kim, spontaneous formation of liquid crystals in ultralarge graphene oxide dispersions, Adv. Funct. Mater. 21 (2011) 2978.
[37] R. Cruz-Silva, A. Morelos-Gomez, H. Kim, H.K. Jang, F. Tristan, S. Vega-Diaz, L.P. Rajukumar, A.L. Elías, N. Perea-Lopez, J. Suhr, M. Endo, M. Terrones, Super-stretchable graphene oxide macroscopic fibers with outstanding knotability fabricated by dry film scrolling, ACS Nano 8 (2014) 5959–5967.
[38] W.S. Hummers, R.E. Offeman, Preparation of graphitic oxide, J Am. Chem. Soc. 80 (1958) 1339.
[39] D. Han, L. Yan, W. Chen, W. Li, Preparation of chitosan/graphene oxide composite film with enhanced mechanical strength in the wet state, Carbohydr. Polym. 83 (2011) 653.
[40] J.I. Paredes, S. Villar-Rodil, A. Martinez-Alonso, J.M.D. Tascón, Graphene oxide dispersions in organic solvents, Langmuir 24 (2008) 10560.
[41] K.N. Kudin, B. Ozbas, H.C. Schniepp, R.K. Prud'homme, I.A. Aksay, R. Car, Raman spectra of graphite oxide and functionalized graphene sheets, Nano Lett. 8 (2008) 36.
[42] F. Emadi, A. Amini, A. Gholami, Y. Ghasemi, Functionalized graphene oxide with chitosan for protein nanocarriers to protect against enzymatic cleavage and retain collagenase activity, Sci. Reports 7 (2017) 42258.
[43] G. Wang, J. Yang, J. Park, X. Gou, B. Wang, H. Liu, J. Yao, Facile synthesis and characterization of graphene nanosheets, J. Phys. Chem. C 112 (2008) 8192.
[44] Y. Guo, X. Sun, Y. Liu, W. Wang, H. Qiu, J. Gao, One pot preparation of reduced graphene oxide (RGO) or Au (Ag) nanoparticle-RGO hybrids using chitosan as a reducing and stabilizing agent and their use in methanol electrooxidation, Carbon 50 (2012) 2513.
[45] X. Lin, X. Shen, Q. Zheng, N. Yousefi, L. Ye, Y.W. Mai, J.K. Kim, Fabrication of highly-aligned, conductive, and strong graphene papers using ultralarge graphene oxide sheets, ACS Nano 6 (2012) 10708.
[46] K.W. Putz, O.C. Compton, C. Segar, Z. An, S.B.T. Nguyen, L.C. Brinson, Evolution of order during vacuumassisted self-assembly of graphene oxide paper and associated polymer nanocomposites, ACS Nano 5 (2011) 6601.
[47] X. Ruan, Y. Chen, H. Chen, G. Qian, R.L. Frost, Sorption behavior of methyl orange from aqueous solution on organic matter and reduced graphene oxides modified Ni-Cr layered double hydroxides, Chem. Eng. J. 297 (2016) 295.
[48] G.K. Ramesha, A.V. Kumara, H.B. Muralidhara, S. Sampath, Graphene and graphene oxide as effective adsorbents toward anionic and cationic dyes, J. Colloid Interface Sci. 361 (2011) 270.
[49] G. Crini, F. Gimbert, C. Robert, B. Martel, O. Adam, N. Morin-Crini, F. De Giorgi, P.M. Badot, The removal of Basic Blue 3 from aqueous solutions by chitosan-based adsorbent: Batch studies, J. Hazardous Mat. 153 (2008) 96.
[50] W. Konicki, M. Aleksandrzak, D. Moszyński, E. Mijowska, Adsorption of anionic Azo-dyes from aqueous solutions onto graphene oxide: equilibrium, kinetic and thermodynamic studies, J. Colloid Interface Sci. 496 (2017) 188.
[51] E. Guibal, P. McCarrick, J.M. Tobin, Comparison of the sorption of anionic dyes on activated carbon and chitosan derivatives from dilute solutions, J. Sep. Sci. Technol. 38 (2003) 12.
[52] G.L. Dotto, L.A.A. Pinto, Adsorption of food dyes acid blue 9 and food yellow 3 onto chitosan: Stirring rate effect in kinetics and mechanism, J. Hazard. Mater. 187 (2011) 164.
[53] M.T. Yagub, T. Kanti, S.S. Afroze, H.M. Ang, Dye and its removal from aqueous solution by adsorption: A review, Adv. Colloid Interface Sci. 209 (2014) 172.
[54] N. Sakkayawong, P. Thiravetyan, W. Nakbanpote, Adsorption mechanism of synthetic reactive dye wastewater by chitosan, J. Colloid Interface Science 286 (2005) 36.
[55] R. Huang, Q. Liu, J. Huo, B. Yang, Adsorption of methyl orange onto protonated cross-linked chitosan, Arabian J. Chem. 10 (2017) 24.
[56] W. Zhang, C. Zhou, W. Zhou, A. Lei, Q. Zhang, Q. Wan, B. Zou, Fast and Considerable Adsorption of Methylene Blue Dye onto Graphene Oxide, Bull. Environ. Contamination Toxicol. 87 (2011) 86.
[57] P. Bradder, S.K. Ling, S. Wang, S. Liu, Dye adsorption on layered graphite oxide, J. Chem. Eng. Data 56 (2011) 138.
[58] D. Robati, B. Mirza, M. Rajabi, O. Moradi, I. Tyagi, S. Agarwal, V.K. Gupta, Removal of hazardous dyes-BR 12 and methyl orange using graphene oxide as an adsorbent from aqueous phase, Chem. Eng. J. 284 (2016) 687.
[59] F. Perreault, A. Fonseca de Faria, S. Nejati, M. Elimelech, Antimicrobial properties of graphene oxide nanosheets: why size matters, ACS Nano 9 (2015) 7226.
[60] M. Kong, X.G. Chen, K. Xing, H.J. Park, Antimicrobial properties of chitosan and mode of action: A state of the art review, Int.. J. Food Microb. 144 (2010) 51.
[61] O. Akhavan, E. Ghaderi, toxicity of graphene and graphene oxide nanowalls against bacteria, ACS Nano 4 (2010) 5731.
[62] H.M. Hegab, A. El Mekawy, L. Zou, D. Mulcahy, C.P. Saint, M. Ginic-Markovic, The controversial antibacterial activity of graphene-based materials, Carbon 105 (2016) 362.
[63] B. Song, P. Xu, G. Zeng, J. Gong, X. Wang, J. Yan, S. Wang, P. Zhang, W. Cao, S. Ye, Modeling the transport of sodium dodecyl benzene sulfonate in riverine sediment in the presence of multi-walled carbon nanotubes, Water Res. 129 (2018) 20.
[64] B. Song, M. Chen, S. Ye, P. Xu, G. Zeng, J. Gong, J. Li, P. Zhang, W. Cao, Effects of multi-walled carbon nanotubes on metabolic function of the microbial community in riverine sediment contaminated with phenanthrene, Carbon 144 (2019) 1.
[65] W. Sun, M. Li, W. Zhang, J. Wei, B. Chen, C. Wang, Sediments inhibit adsorption of 17β-estradiol and 17α-ethinylestradiol to carbon nanotubes and graphene oxide, Environ. Sci.: Nano 4 (2017) 1900.
[66] Z. Hu, Z. Tang, X. Bai, J. Zhang, L. Yu, H. Cheng, Aggregation and resuspension of graphene oxide in simulated natural surface aquatic environments, Environ. Pollut. 205 (2015) 161.
[67] M.F.L. De Volder, S.H. Tawfick, R.H. Baughman, A.J. Hart, Carbon nanotubes: present and future commercial applications, Science 339 (2013) 535.